NASA Technical Memorandum 101571

AN INVESTIGATION OF THE "OVERLAP" BETWEEN THE STATISTICAL DISCRETE GUST AND THE POWER SPECTRAL DENSITY ANALYSIS METHODS

Boyd Perry III, Anthony S. Pototzky, and Jessica A. Woods

(NASA-TM-101571) AN INVESTIGATION OF THE OVERLAP BETWEEN THE STATISTICAL DISCRETE GUST AND THE POWER SPECTRAL DENSITY ANALYSIS METHODS (NASA. Langley Research Center) 15 p CSCL 01C G3/05

N89-24310

Unclas 0216763

APRIL 1989

National Aeronautics and Space Administration

Langley Research Center
Hampton, Virginia 23665-5225

An Investigation of the "Overlap" Between the Statistical-Discrete-Gust and the Power-Spectral-Density Analysis Methods

by

Boyd Perry III*
NASA Langley Research Center
Hampton, Virginia 23665-5225

and

Anthony S. Pototzky** and Jessica A. Woods***
Planning Research Corporation
Aerospace Technologies Division
Hampton, Virginia 23666

Abstract

This paper presents the results of a NASA investigation of a claimed "Overlap" between two gust response analysis methods: the Statistical Discrete Gust (SDG) Method and the Power Spectral Density (PSD) Method. The claim is that the ratio of an SDG response to the corresponding PSD response is 10.4. Analytical results presented in this paper for several different airplanes at several different flight conditions indicate that such an "Overlap" does appear to exist. However, the claim was not met precisely: a scatter of up to about 10% about the 10.4 factor can be expected.

Introduction

The U.S. Federal Aviation Administration (FAA) has formed an *ad hoc* international committee of gust specialists which draws its membership from domestic and foreign civil airworthiness authorities, airframe manufacturers, and research laboratories. The committee's work is part of an on-going effort to rationalize and improve the gust criteria applied by U.S. and European airworthiness authorities. The effort includes the investigation of candidate analysis methods for gust-loads certification.

The Statistical Discrete Gust (SDG) Method of computing gust loads (ref. 1) was identified by the *ad hoc* committee as a candidate for further investigation. The SDG Method has offered a significant advantage over the Power Spectral Density (PSD) Method because the SDG Method computes time-correlated gust loads directly. In reference 2 J. G. Jones, developer of the SDG Method, claims that, under certain circumstances, the SDG and PSD Methods produce essentially the same numerical results, or that "... the former is essentially simply an approximate numerical implementation of the latter." Jones refers to this situation as the "SDG - PSD Overlap."

In response to a recommendation from the *ad hoc* committee, in the fall of 1986 the FAA requested assistance from the National Aeronautics and Space Administration (NASA) to investigate Jones' claim of the "SDG - PSD Overlap." Over the course of the following 24 months NASA performed the requested investigation and the purpose of this paper is to report the results of that investigation.

Descriptions of Analysis Methods

Both the Statistical Discrete Gust Method and the Power Spectral Density Method compute the response of an airplane to atmospheric turbulence. The former is performed in the time domain; the latter in the frequency domain. The input to both methods is the same numerical description of the airplane. This section of the paper provides a heuristic outline of each method and comments on the computer implementation of each.

Statistical Discrete Gust (SDG) Method

The objective of the SDG Method is to determine analytically the maximum, or worst-case, responses of an airplane to discrete gusts representative of atmospheric turbulence. The Method is carried out in the time domain through the calculation of response time histories. The Method was originally developed more than 15 years ago by Jones (ref. 1). Over the course of those years, and continuing into the present, the Method has undergone refinements and improvements (refs. 2 through 6).

The SDG Method is based on the assumption that

---

* Aerospace Engineer
** Engineering Specialist, Member AIAA
*** Structures Engineer, Member AIAA

atmospheric turbulence is comprised of a family of discrete equiprobable smoothly-varying ramp-held gusts whose maximum magnitudes ($\bar{w}_g$) vary as indicated by the dashed envelope in figure 1 and as defined by the following equation

$$\bar{w}_g(H) = U_0 H^k \quad (\text{for } 0 \le H \le L) \tag{1}$$

where U_0 is a gust intensity parameter, H is the gradient distance, k is a fractional exponent, and L is the scale of turbulence.

Each discrete gust is defined by a transient portion (the first half of a one-minus-cosine wave) followed by a steady-state portion (whose value is equal to the value of the transient portion at the end of the transient). The length of the transient is the gradient distance. The expression for one member of the family of gusts is

$$w_g(s, H) = \begin{cases} \dfrac{\bar{w}_g(H)}{2}\left(1 - \cos\left(\dfrac{\pi s}{H}\right)\right) & (\text{for } 0 \le s \le H) \\ \bar{w}_g(H) & (\text{for } H < s \le L) \end{cases} \tag{2}$$

where s is distance and is related to time through the velocity, V.

In the implementation of the Method, an airplane is subjected to the following inputs, applied one at a time:

- all possible single gusts
- all possible combinations of two gusts with all possible "spacings" (defined below) between the gusts
- all possible combinations of three gusts with all possible combinations of "spacing" between the gusts

  .
  .
  .
- all possible combinations of n gusts with all possible combinations of "spacing" between the gusts.

In general, time histories of each airplane response quantity due to each of the (extremely large number of) inputs is examined in order to find the worst-case response (that is, the largest positive or negative peak value) of each response quantity. The combination of gusts that produces the worst-case response is referred to as the Critical Gust Pattern.

Figure 2 contains a sketch of a combination of three gusts, labelled ①②③, in the time domain. Quantities τ_1 and τ_2 in the figure represent "spacings" in time between the completion of the transient of one gust and the start of the transient of the next. As indicated in the figure by the direction of the arrows, τ_1 and τ_2 are positive; however, τ_1 and τ_2 may also be negative. When either τ_1 or τ_2 is negative, the associated gusts are said to overlap one another.

For an airplane modelled as a linear system, this extremely large number of inputs may be reduced to a manageable number by taking advantage of superposition, as described in reference 3. With superposition, worst-case responses to combinations of two or more gusts are determined by the responses to single gusts only. Thus, from a computer-implementation point of view, the analytical model of the airplane need never be subjected to the critical gust pattern in order to obtain the worst-case response. However, with proper bookkeeping and by retaining the necessary intermediate results, once the overall worst-case response has been determined, the critical gust pattern may be constructed from the single gusts.

As the number of gusts in a combination increases from one to n, the probability of encountering that combination in the assumed atmospheric turbulence decreases, and this decrease in probability is accounted for analytically through the use of amplitude reduction factors. The amplitude reduction factors reduce the magnitudes of the inputs (and for a linear system, reduce the magnitudes of the responses by the same ratio), thereby bringing the responses to all single gusts and the responses to all combinations of gusts to the same level of probability of occurrence.

The following equation illustrates how the overall worst-case response is determined.

$$\bar{\gamma} = \max\begin{cases} p_1 \gamma_1 \\ p_2 \gamma_2 \\ p_3 \gamma_3 \\ \vdots \\ p_n \gamma_n \end{cases} \tag{3}$$

The γ_i's are the individual worst-case responses to a combination of i gusts; the p_i's are the corresponding amplitude reduction factors. The overall worst-case response, $\bar{\gamma}$, is the worst of the worst, or the maximum of the products of the γ_i's and their corresponding p_i's. The critical gust pattern is constructed by summing single ramp inputs associated with $\bar{\gamma}$.

Two implementations of the SDG Method will be

addressed in this paper. Jones refers to these implementations as "Method 1" and "Method 2." Method 1 contains simplifying assumptions about the characteristics of critical gust patterns and approximations in the computation of the amplitude reduction factors that make it computationally faster, but more restrictive and less exact than Method 2. Method 2 is more general and for this reason it will be discussed first.

Method 2. In Method 2 there are no restrictions concerning the characteristics of the critical gust patterns. Critical gust patterns are comprised of single gusts whose magnitudes may be negative or positive (representing either up or down gusts) in any order, and whose spacing in time may be negative or positive (representing subsequent gusts which either do or do not overlap each other).

The amplitude reduction factors are computed based on the following formula (ref. 6)

$$p_1 = 1$$

$$p_i = \frac{1}{0.88\sqrt{\frac{I_i}{I_1}}} \quad \text{for } i \geq 2 \tag{4}$$

where

$$I_i = \int_0^{s_i} \left(\frac{d^{5/6} v(s)}{ds^{5/6}} \right)^2 ds \tag{5}$$

and where v(s) is a gust pattern made up of i individual ramps, s is distance, and s_i is the distance at the completion of the transient of the i-th ramp. Numerical evaluation of the fractional derivative in equation (5) is outlined in the appendix of reference 5.

Method 1. In Method 1 there are restrictions concerning the characteristics of the critical gust patterns. Critical gust patterns are comprised of single gusts whose magnitudes must have alternating negative and positive signs (representing alternating up and down gusts), and whose spacing in time must be positive (representing subsequent gusts which do not overlap each other).

In Method 1 the amplitude reduction factors are computed based on the following formula (ref. 6)

$$p_1 = 1$$

$$p_i = \frac{1}{0.88\sqrt{i}} \quad \text{for } i \geq 2 \tag{6}$$

which is an approximation to equation (4). Because Method 1 is less general than Method 2, there exist conditions where the two cases predict almost identical amplitude reduction factors. For a gust pattern which satisfies the Method 1 restrictions, the radical in equation (4) consistently reduces to the radical in equation (6) and the Method 2 results are almost identical to those of Method 1.

A recommended way to implement Method 1 is to compute worst-case responses by taking advantage of superposition and then to examine the resulting critical gust patterns for possible violation of the restrictions. If there are no violations of restrictions, then the answers obtained are valid Method 1 answers. If there are violations of restrictions then the answers are not valid, but there are three alternatives:

(1) abandon Method 1 and implement Method 2;

(2) abandon Method 1 and implement Method 1A;

(3) continue with Method 1 but abandon superposition as a technique for finding the worst-case responses.

Alternative (1) was discussed in the previous section; alternative (2) will be discussed in the next section. Alternative (3) involves subjecting the airplane to an extremely large number of inputs and then choosing the worst -case response. This large number of inputs is the subset of all possible inputs which does not have Method 1 violations. Alternative (3) is not practical to implement because of the large number of inputs required.

Method 1A. If there are violations of the Method 1 restrictions, then an empirical correction factor may be applied to the (necessarily invalid) answers to reduce the magnitudes of the worst-case responses. The application of this empirical correction is referred to by Jones as "Method 1A" (ref. 6) and may be applied when the critical gust pattern has overlapping gusts in the same direction; it does not apply under several other possible conditions:

- when the critical gust pattern has overlapping gusts in the opposite direction
- when the critical gust pattern has non-overlapping gusts in the same direction
- when the critical gust pattern has multiply-overlapping gusts in the same or opposite directions

If any of these three conditions exist, then Method 1A may not be used and the only correct way to implement Method 1 is to abandon superposition and to subject the airplane to an extremely large number of inputs.

Power Spectral Density (PSD) Method

The Power Spectral Density (PSD) Method was first applied to the airplane turbulence response problem almost 40 years ago (ref. 7). Since that time the PSD Method has become so widely-accepted that the Federal Aviation Regulations (specifically, FAR 25.305(d)) require that, unless a more rational method is used, an airplane manufacturer must use the PSD Method to establish the dynamic response of its airplanes to atmospheric turbulence.

The fundamental quantity of the PSD Method is the power spectral density function, or, power spectrum. A power spectrum contains all the statistical information describing a random process, including the root-mean-square (rms) value. The random processes in question in the present application are atmospheric turbulence (the input random process) and airplane responses (the output random processes). The input is assumed Gaussian, and because the system is assumed linear, the output is also Gaussian. It is assumed that the turbulence is one-dimensional (that is, uniform across the span), homogeneous, isotropic, and "frozen" in space during the time it takes the airplane to traverse its own length.

The input and output power spectral density functions are related to each other through the square of the modulus of the airplane frequency response function, as given by the following equation

$$\Phi_y(\omega) = \Phi_{w_g}(\omega)\left|H_y(i\omega)\right|^2 \tag{7}$$

where $\Phi_y(\omega)$ is the airplane response power spectrum and $\Phi_{w_g}(\omega)$ is the atmospheric turbulence power spectrum. The airplane frequency response function, $H_y(i\omega)$, represents the response (magnitude and phase), over a range of frequencies, of quantity y to a unit sinusoidal gust velocity. $H_y(i\omega)$ contains all the dynamics of the airplane (rigid-body modes and elastic modes).

For present purposes, von Karman's form of $\Phi_{w_g}(\omega)$ was chosen and is given by the following equation (ref. 8)

$$\Phi_{w_g}(\omega) = \frac{\sigma^2_{w_g} L}{\pi V} \frac{1 + \frac{8}{3}\left(1.339\,\frac{L}{V}\omega\right)^2}{\left[1 + \left(1.339\,\frac{L}{V}\omega\right)^2\right]^{11/6}} \tag{8}$$

Figure 3 contains a log-log plot of $\Phi_{w_g}(\omega)$ as a function of ω. For illustration purposes the quantity σ_{w_g} and the ratio L / V were chosen to be unity. At low values of frequency the function asymptotically approaches a constant value ($\sigma^2_{w_g} L / \pi V$); at high values of frequency the function asymptotically approaches zero as $\omega^{-5/3}$. At intermediate values of frequency the function makes a transition between the low- and high-frequency asymptotes and reaches a maximum, referred to as the "knee." The corresponding frequency is referred to as the "knee frequency," ω_{knee}, where

$$\omega_{knee} \equiv 0.457\frac{V}{L} \tag{9}$$

The root-mean-square values of random processes w_g and y may be obtained by performing the following operations

$$\sigma_{w_g} = \left[\int_0^\infty \Phi_{w_g}(\omega)\,d\omega\right]^{\frac{1}{2}} \tag{10}$$

and

$$\sigma_y = \left[\int_0^\infty \Phi_y(\omega)\,d\omega\right]^{\frac{1}{2}} \tag{11}$$

$\bar{A}$ is the normalized response quantity, defined as the ratio of the rms of the output to the rms of the input

$$\bar{A} = \frac{\sigma_y}{\sigma_{w_g}} \tag{12}$$

"SDG - PSD Overlap"

Jones claims that, under certain circumstances, the SDG and PSD Methods produce essentially the same numerical results (ref. 2) and he refers to this situation as the "SDG - PSD Overlap." The quantitative definition of the Overlap is given by the equation

$$\bar{\gamma} = 10.4\,\bar{A} \tag{13}$$

where $\bar{\gamma}$ is defined by equation (3) and $\bar{A}$ is defined by equation (12).

The "certain circumstances" under which equation (13) is valid are summarized in Table I. Quantities from the SDG Method are found in equations (1) and (2); quantities from the PSD Method, in equations (8) and (9). The value 1/3 for exponent k in equation (1) corresponds to the -5/3 high-frequency asymptote of the von Karman power spectrum in equation (8). For both the SDG and PSD Methods, unit gust velocities and the standard value of scale of turbulence are used. In addition, in the PSD Method there is a requirement that the frequency of the short-period mode be much greater than the knee frequency

of the von Karman power spectrum. With these conditions met, Jones claims that the "10.4 factor" of equation (13) will be obtained if SDG and PSD analyses are performed for the same vehicle.

Approach for Verification of the "Overlap"

The approach taken in the NASA investigation of the "SDG - PSD Overlap" was to perform SDG and PSD analyses for several airplanes at different flight conditions and to compare the corresponding responses from each Method to see if the "10.4 factor" was obtained. To maintain impartiality and independence during the investigation, NASA wrote its own computer codes and chose its own configurations, flight conditions, and responses quantities. In an attempt to define quantitatively the limits of the "Overlap," several parameters were varied.

Both rigid-body analyses and fully-flexible analyses were performed: rigid-body analyses using Method 1 only for five configurations; fully-flexible analyses using Methods 1 and 2 for one configuration. All were symmetric longitudinal analyses with the vertical component of atmospheric turbulence as the disturbance quantity.

Rigid-Body Analyses

For the rigid-body analyses, the short-period approximation to the longitudinal small-perturbation equations of motion (ref. 9) were used. These equations are written in stability axes and employ stability derivatives to approximate the effects of unsteady aerodynamics

$$\left[C_\alpha \; C_\theta\right]\begin{Bmatrix}\alpha\\ \theta\end{Bmatrix} = \{C_g\}\frac{w_g}{V} \tag{14}$$

where α and θ are the rigid-body degrees of freedom, w_g is gust velocity, C_α, C_θ, and C_g are the corresponding coefficients. Response quantities for these analyses include pitch rate, θ, and vertical acceleration at the vehicle center of gravity, Δn, which is expressed in g units as

$$\Delta n = \frac{V}{g}(\dot{\alpha} - \dot{\theta}) \tag{15}$$

Fully-Flexible Analyses

For the fully-flexible analyses, the equations of motion of a flexible vehicle were used. Aerodynamic characteristics were determined by a doublet-lattice unsteady aerodynamics code (ref. 10). The equations of motion are derived through a modal approach using Lagrange's equations, resulting in linearized small-perturbation matrix equations of the form

$$[M]\{\ddot{q}\} + [D]\{\dot{q}\} + [K]\{q\} + \tfrac{1}{2}\rho V^2[Q]\{q\} = \tfrac{1}{2}\rho V^2\{Q_g\}w_g \tag{16}$$

where M, D, and K are respectively the generalized mass, damping and stiffness matrices, Q and Q_g are the generalized aerodynamic force matrices due to vehicle motion and gust, q is the vector of generalized coordinates, ρ is fluid density, V is velocity and w_g is gust velocity.

Response quantities included angular rates and linear accelerations, shear forces, bending moments, and torsion moments at several locations on the example configuration. The rates and accelerations are obtained by weighting the generalized-coordinate rates and accelerations by modal slopes and deflections. The forces and moments are obtained by the summation of forces method of computing dynamic loads (ref.11). These dynamic loads are comprised of inertia, motion-aerodynamic, and gust-aerodynamic components as indicated by the following equation

$$\{\bar{L}\} = [\bar{M}]\{\ddot{q}\} + \tfrac{1}{2}\rho V^2[\bar{Q}]\{q\} + \tfrac{1}{2}\rho V^2\{\bar{Q}_g\}w_g \tag{17}$$

where $\bar{L}$ is a vector of dynamic loads, $\bar{M}$ is the inertial dynamic loads matrix, $\bar{Q}$ and $\bar{Q}_g$ are the aerodynamic dynamic loads matrices due to vehicle motion and gust, q is the vector of generalized coordinates, ρ is fluid density, V is velocity and w_g is gust velocity.

Numerical Results

Unless specifically identified as being otherwise, all numerical results presented in this section of the paper meet the conditions of "SDG-PSD Overlap" as defined in Table I.

Results from Rigid-Body Analyses

In performing the rigid-body analyses, five different configurations, spanning a wide range of vehicle types, weights, and flight conditions, were used. Table II summarizes the characteristics of these configurations.

For each configuration the PSD Method and Method 1 of the SDG Method were performed using the short-period approximation to the equations of motion. For the PSD Method 250 points were used in the numerical integration of equations (10) and (11). For the SDG

Method, the vehicles were each subjected to about 50 single ramps. Table III and figure 4 summarize these results. As indicated in the table, all critical gust patterns were comprised of either one (n=1) or two (n=2) single gusts. None of the n=2 cases had either overlapping gusts in the critical pattern or subsequent gusts in the same direction. Thus, the characteristics of the critical gust patterns for all cases comply with the restrictions which apply to Method 1, and Method 1A was not required.

In the last column of the table it is seen that all ratios of $\bar{\gamma}/\bar{A}$ fall between 9.51 (8.6% below 10.4) and 11.13 (7.0% above 10.4). The mean value of the ratios is 10.32, with a standard deviation of 0.56.

Variation of the $\omega_{sp}/\omega_{knee}$ ratio. An investigation was performed to determine the effect of the $\omega_{sp}/\omega_{knee}$ ratio on the resulting $\bar{\gamma}/\bar{A}$ ratios. Using configuration 2, the value of $C_{m\alpha}$ was artificially varied in order to vary the short-period frequency, and the SDG and PSD analyses were re-performed. Eight additional values of $C_{m\alpha}$ were chosen, four above and four below the nominal value, resulting in about a factor-of-five reduction and a factor-of-five increase in short-period frequency. Results of this investigation are presented in figure 5.

Figure 5 contains a semi-log plot of the $\bar{\gamma}/\bar{A}$ ratio for pitch-rate response as a function of the $\omega_{sp}/\omega_{knee}$ ratio for configuration 2. At values of the $\omega_{sp}/\omega_{knee}$ ratio below ten the $\bar{\gamma}/\bar{A}$ ratios depart by almost 20% from 10.4; at values of the $\omega_{sp}/\omega_{knee}$ ratio above ten the $\bar{\gamma}/\bar{A}$ ratios remain very close to 10.4. These results indicate that the $\bar{\gamma}/\bar{A}$ ratio is, in fact, a function of the $\omega_{sp}/\omega_{knee}$ ratio and they quantify Jones' claim that ω_{sp} should be much greater than ω_{knee}.

Results from Fully-Flexible Analyses

In performing the fully-flexible analyses, a single configuration was used: the NASA DAST ARW-2 vehicle. This vehicle is a Firebee II target drone with its standard wings replaced with aeroelastic research wings. For these analyses two rigid-body (plunge and pitch) and four symmetric flexible modes were used. The eigenvalues at the analysis condition of 0.7 Mach number and 15,000 feet altitude are plotted in figure 6. For this configuration, the short-period frequency is 21.7 times the knee frequency.

The PSD Method and Methods 1 and 2 of the SDG Method were performed using the flexible-airplane equations of motion. For the PSD Method 1000 points were used in the numerical integration of equation (11). For the SDG Method, the vehicles were each subjected to 50 single ramps. Results from Methods 1 and 2 will be discussed separately.

SDG Method 1. Table IV and figure 7 summarize the PSD and SDG Method 1 results. As indicated in the table, due to the presence of flexible modes in the equations of motion, the resulting critical gust patterns are significantly more complicated than they were for the rigid-body analyses. Depending on the response, critical gust patterns are comprised of from three to six single ramps. In addition, for half of the responses, the critical gust patterns contain overlapping ramps and subsequent ramps in the same direction, indicating that Method 1A must be attempted for these responses.

The single asterisk to the left of Table IV indicates that Method 1 was used to determine the SDG response; the double asterisk, that Method 1A was used. SDG responses for eight of the ten quantities could be determined using either Method 1 or Method 1A. As indicated in the table, for two of the quantities (mid torsion moment and c.g. vertical acceleration) neither Method 1 nor Method 1A could supply valid SDG responses because of multiply overlapping ramps in their respective critical gust patterns. In this case, then, the only correct way to obtain SDG responses using Method 1 is to abandon superposition and to subject the configuration to an extremely large number of inputs, which was not attempted

For the eight quantities for which SDG responses could be obtained, all ratios of $\bar{\gamma}/\bar{A}$ fall between 8.80 (15.4% below 10.4) and 11.03 (6.1% above 10.4). The mean value of the ratios is 10.26, with a standard deviation of 0.81.

SDG Method 2. Table V and figure 7 summarize the PSD and SDG Method 2 results. Again, due to the presence of flexible modes in the equations of motion, the resulting critical gust patterns are significantly more complicated than they were for the rigid-body analyses. Depending on the response, critical gust patterns are comprised of from three to ten single ramps. The same five quantities which had critical gust patterns violating Method 1 restrictions show the same trend in the Method 2 results. However, because Method 2 is more general than Method 1, answers have been, and can always be, computed for all ten response quantities.

As indicated in the last column of the table, all ratios of $\bar{\gamma}/\bar{A}$ fall between 8.49 (18.4% below 10.4) and 11.50 (10.6% above 10.4). The mean value of the ratios is 10.45, with a standard deviation of 0.91.

Figure 8 contains an example of the kind of time-correlated gust loads available from the SDG Method.

Part (a) of the figure contains the critical gust pattern for mid bending moment as determined by Method 2. It is comprised of three single ramps; the last two overlap each other and are in the same direction. Part (b) contains the corresponding mid bending moment response, with peak value occurring at about 1.4 seconds into the time history. Part (c) contains the mid-torsion-moment response resulting from the critical gust pattern for mid-bending moment. Time histories (b) and (c) are time-correlated gust loads.

Observations

Table VI contains a summary of the sizes of the problems solved and the computer resources required to solve those problems. Problem sizes have been expressed as the sum of the order of the linear system plus the number of outputs. All computer resources are for the NASA-Langley CDC Cyber computers. The term "computational cost" is defined to be the product of CPU time and field length. Several observations can be made:

(1) for rigid-body and fully-flexible analyses, the computational cost of performing an SDG analysis is significantly (twenty to thirty times) larger than that of a PSD analysis;

(2) the computational cost of an SDG Method 2 analysis is about twice that of an SDG Method 1 analysis.

Table VI also contains a summary of the statistics of the $\overline{\gamma} / \overline{A}$ ratios for the problems solved:

(1) the mean values of the $\overline{\gamma} / \overline{A}$ ratios remain within 2% of 10.4 for all implementations of the SDG Method (Methods 1, 1A, and 2);

(2) the standard deviations of the $\overline{\gamma} / \overline{A}$ ratios about their respective means increase with the inclusion of flexible modes in the equations of motion.

Concluding Remarks

This paper has presented the results of a recent NASA investigation of the "SDG - PSD Overlap." SDG and PSD analyses were performed for several airplanes at different flight conditions and responses from each Method were compared to see if the "10.4 factor" was obtained. Both rigid-body analyses and fully-flexible analyses were performed. In addition, an approximate form (Method 1) and a more accurate form (Method 2) of the SDG Method were implemented and investigated.

During the investigations several parameters were varied in an attempt to define quantitatively the limits of the "Overlap." Based on both the rigid-body and the fully-flexible results, an "SDG - PSD Overlap" does appear to exist. However, this overlap appears to be characterized, not by a "10.4 factor," but rather by a "10.4 plus-or-minus-approximately-five-percent factor" when rigid-body equations are involved, and by a "10.4 plus-or-minus-approximately-ten-percent factor" when fully-flexible equations are involved. In addition, there is no guarantee that an SDG Method 1 analysis will produce valid answers. Complicated critical gust patterns may require abandoning superposition, resulting in the requirement that the configuration be subjected to an extremely large number of inputs in order to obtain answers.

Other significant findings were the relative computational costs of performing analyses using the PSD Method and both SDG Methods. An SDG Method 1 analysis costs between twenty and thirty times as much as a PSD analysis; an SDG Method 2 analysis costs twice that of an SDG Method 1 analysis.

References

1. Jones, J. G.: Statistical Discrete Gust Theory for Aircraft Loads. RAE Technical Report 73167, 1973.

2. Jones, J. G.: A Unified Procedure for Meeting Power-Spectral-Density and Statistical-Discrete-Gust Requirements for Flight in Turbulence. AIAA Paper No. 86-1011-CP, May 19-21, 1986.

3. Jones, J. G.: On the Formulation of Gust-Load Requirements in Terms of the Statistical Discrete Gust Method. RAE Technical Memo FS 208, 1978.

4. Jones, J. G.: Summary Notes on Statistical Discrete Gust Method. RAE Technical Memo FS 323, 1980.

5. Jones, J. G.: An Equivalence Between Deterministic and Probabilistic Design Criteria for Linear Systems. Journal of Sound and Vibration, Vol. 125, No. 2, 1988, pp. 341-356.

6. Jones, J. G.: Correspondence sent to the authors, available upon request.

7. Clementson, G. C.: An Investigation of the Power Spectral Density of Atmospheric Turbulence. Ph.D. Thesis, Massachusetts Institute of Technology, 1950.

8 Houbolt, J. C.; Steiner, R.; and Pratt, K. G.: Dynamic Response of Airplanes to Atmospheric Turbulence Including Flight Data on Input and Response. NASA Technical Report R-199, 1964.

9. Etkin, Bernard: *Dynamics of Flight: Stability and Control*. John Wiley & Sons, 1959.

10. Geising, J. P.; Kalman, T. P.; and Rodden, W. P.: Subsonic Unsteady Aerodynamics for General Configurations, Part I: Direct Application of the Nonplanar Doublet Lattice Method. AFFDL-TR-71-5, 1971.

11. Pototzky, A. S.; and Perry, B. III: New and Existing Techniques for Dynamic Loads Analysis of Flexible Airplanes. Journal of Aircraft, Vol. 23, No. 4, April 1986, pp. 340-347.

Table I. - Conditions for the "SDG - PSD Overlap"

SDG Quantities (Refer to equations (1) and (2))	PSD Quantities (Refer to equations (8) and (9))
$k = \frac{1}{3}$	von Karman form of $\Phi_{w_g}(\omega)$
$U_0 = 1$ foot per second	$\sigma_{w_g} = 1$ foot per second
$L = 2500$ feet	$L = 2500$ feet
------	$\omega_{\text{short period}} >> \omega_{\text{knee}}$

Table II. - Example Configurations for Rigid-Body Analyses

Configuration Number	Vehicle	Fight Condition		Short Period Frequency, ω_{sp} radians/second	$\frac{\omega_{sp}}{\omega_{knee}}$
		Mach No.	Altitude		
1	NASA DAST ARW-2 (Firebee II Drone)	0.70	15,000 ft.	3.44	28.8
2	Etkin Example Transport	0.74	30,000 ft.	1.44	10.8
3	OMAC Laser 300	0.33	Sea Level	3.87	58.2
4	Sabreliner (without active controls)	0.50	20,000 ft.	2.14	22.6
5	Sabreliner (with active controls)	0.50	20,000 ft.	1.89	19.9

Table III. - Summary of SDG (Method 1) and PSD Results for Rigid-Body Analyses

Configuration Number	Response Quantity (units)	PSD Result $\bar{X}$ (units)/fps	SDG Results: Critical Gust Pattern n	Overlap	Direction	SDG Results $\bar{Y}$ (units)	$\frac{\bar{Y}}{\bar{X}}$
1	Pitch rate, $\dot{\theta}$ (radians per second)	0.002062	2	No	Opp.	0.02172	10.53
	c.g. vert. accel., Δn (g's)	0.02827	2	No	Opp.	0.3041	10.76
2	Pitch rate, $\dot{\theta}$ (radians per second)	0.0006212	1	n/a	n/a	0.006913	11.13
	c.g. vert. accel., Δn (g's)	0.01546	1	n/a	n/a	0.1511	9.77
3	Pitch rate, $\dot{\theta}$ (radians per second)	0.005368	1	n/a	n/a	0.05579	10.39
	c.g. vert. accel., Δn (g's)	0.02412	2	No	Opp.	0.2584	10.71
4	Pitch rate, $\dot{\theta}$ (radians per second)	0.001151	1	n/a	n/a	0.01231	10.69
	c.g. vert. accel., Δn (g's)	0.01936	1	n/a	n/a	0.1842	9.51
5	Pitch rate, $\dot{\theta}$ (radians per second)	0.0008433	1	n/a	n/a	0.009133	10.83
	c.g. vert. accel., Δn (g's)	0.01994	1	n/a	n/a	0.1947	9.77
	Control surf. defl., δ (radians)	0.0003686	1	n/a	n/a	0.003573	9.69

Mean: 10.32
Std. Dev.: 0.56

Table IV. - Summary of SDG (Methods 1 & 1A) and PSD Results for Fully-Flexible Analyses

DAST ARW-2
Mach Number = 0.7 Altitude = 15, 000 ft
$\omega_{sp}/\omega_{knee}$ = 21.7

	Response Quantity (units)	PSD Result $\bar{X}$ (units)/fps	SDG Results: Critical Gust Pattern n	Overlap	Direction	SDG Results $\bar{Y}$ (units)	$\frac{\bar{Y}}{\bar{X}}$
**	Outboard Shear Force (pounds)	0.6223	4	Yes	Same	6.611	10.62
*	Outboard Bending Moment (foot-pounds)	0.2153	3	No	Opp.	2.285	10.61
*	Outboard Torsion Moment (foot-pounds)	0.2366	3	No	Opp.	2.608	11.03
**	Mid Shear Force (pounds)	8.428	3	Yes	Same	92.96	11.03
**	Mid Bending Moment (foot-pounds)	19.41	3	Yes	Same	207.5	10.69
†	Mid Torsion Moment (foot-pounds)	2.657	4	Yes	Same	____	____
*	Pitch Rate, c.g. (radians per sec)	0.009581	5	No	Opp.	0.09468	9.88
†	Vertical Acceleration, c.g. (feet per sec^2)	3.515	6	Yes	Same	____	____
*	Vertical Acceleration, y = 82 (feet per sec^2)	156.6	3	No	Opp.	1378.	8.80
*	Vertical Acceleration, y = 84 (feet per sec2)	191.7	4	No	Opp.	1804.	9.41

* SDG Method 1
** SDG Method 1A
† No solution possible via superposition

Mean: 10.26
Std. Dev.: 0.81

Table V. - Summary of SDG (Method 2) and PSD Results for Fully-Flexible Analyses

DAST ARW-2
Mach Number = 0.7 Altitude = 15, 000 ft
$\omega_{sp}/\omega_{knee}$ = 21.7

Response Quantity (units)	PSD Result $\frac{A}{}$ (units)/fps	SDG Results				$\frac{T}{A}$
		Critical Gust Pattern			T (units)	
		n	Overlap	Direction		
Outboard Shear Force (pounds)	0.6223	4	Yes	Same	6.400	10.28
Outboard Bending Moment (foot-pounds)	0.2153	3	No	Opp.	2.385	11.08
Outboard Torsion Moment (foot-pounds)	0.2366	3	No	Opp.	2.720	11.50
Mid Shear Force (pounds)	8.428	3	Yes	Same	94.82	11.25
Mid Bending Moment (foot-pounds)	19.41	3	Yes	Same	212.7	10.96
Mid Torsion Moment (foot-pounds)	2.657	4	Yes	Same	28.54	10.74
Pitch Rate, c.g. (radians per sec)	0.009581	5	No	Opp.	0.1015	10.59
Vertical Acceleration, c.g. (feet per sec^2)	3.515	10	Yes	Same	29.85	8.49
Vertical Acceleration, y = 82 (feet per sec^2)	156.6	4	No	Opp.	1478.	9.44
Vertical Acceleration, y = 84 (feet per sec^2)	191.7	4	No	Opp.	1941.	10.13

Mean: 10.45
Std. Dev.: 0.91

Table VI. - Summary of SDG - PSD Comparisons

Type of Analysis	Problem Size	Computer Resources				$\frac{T}{A}$ Statistics	
		PSD		SDG			
		CPU Time (sec)	Field Length	CPU Time	Field Length	Mean	Standard Deviation
Rigid-Body (Method 1)	4	4	62K	37	137K	10.32	0.56
Fully-Flexible (Method 1)	52	134	170K	2700	236K	10.26	0.81
Fully-Flexible (Method 2)	52	134	170K	4500	364K	10.45	0.91

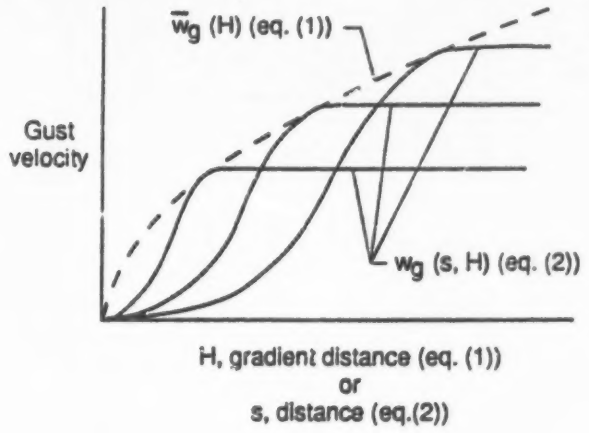

Figure 1. - Family of equi-probable smoothly -varying ramp-hold gusts for SDG Method.

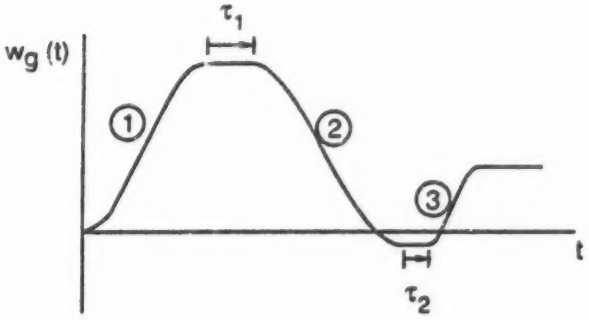

Figure 2. - Combination of three single gusts.

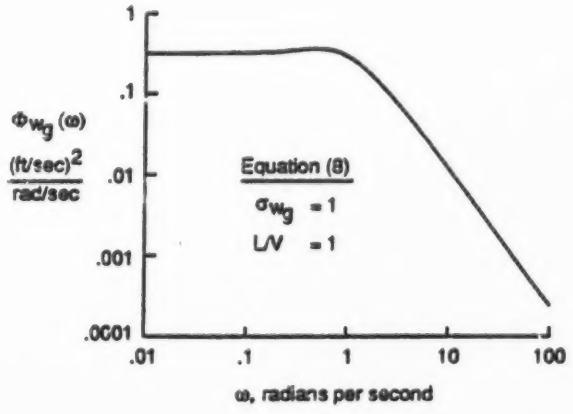

Figure 3. - Von Karman power spectral density function.

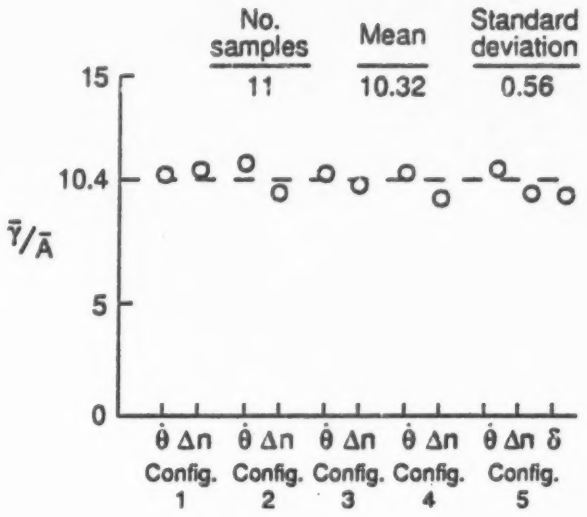

Figure 4. - Comparison of SDG (Method 1) and PSD results for rigid-body analyses.

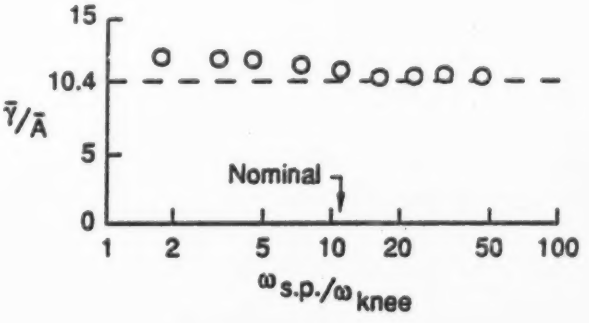

Figure 5. - Comparison of SDG (Method 1) and PSD results for rigid-body analyses as a function of frequency ratio. Configuration 2. Pitch-rate response.

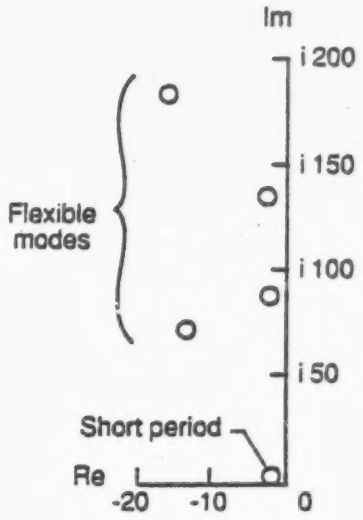

Figure 6. - Eigenvalues of DAST ARW-2 configuration. Mach number 0.7, Altitude 15,000 feet.

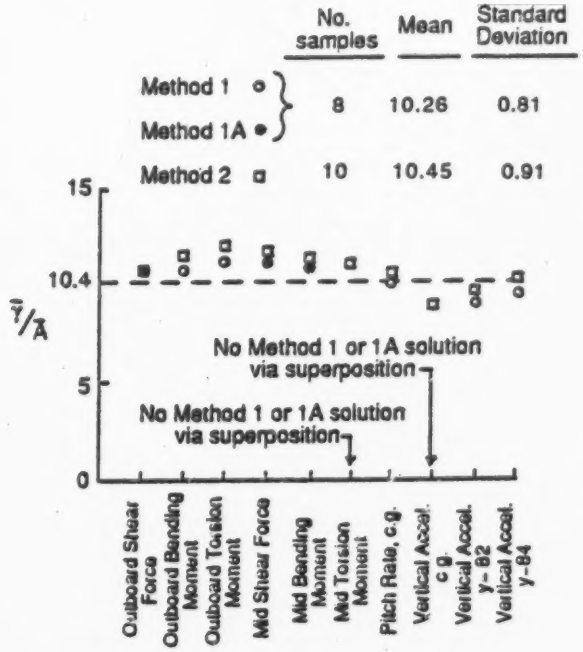

Figure 7. - Comparison of SDG (Methods 1, 1A, and 2) and PSD results for fully-flexible analyses. DAST ARW-2 configuration. Mach number 0.7, Altitude 15,000 feet.

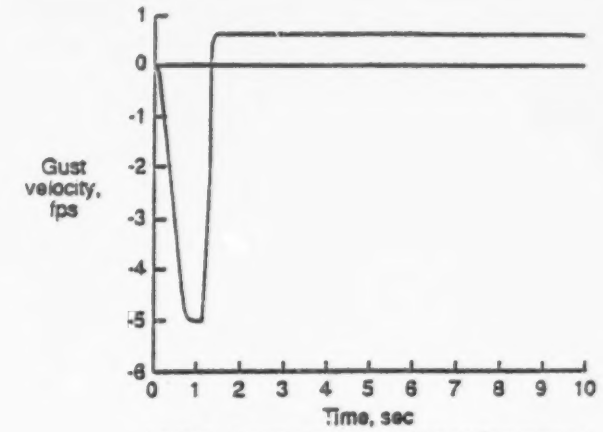

(a) Critical gust pattern for mid bending moment

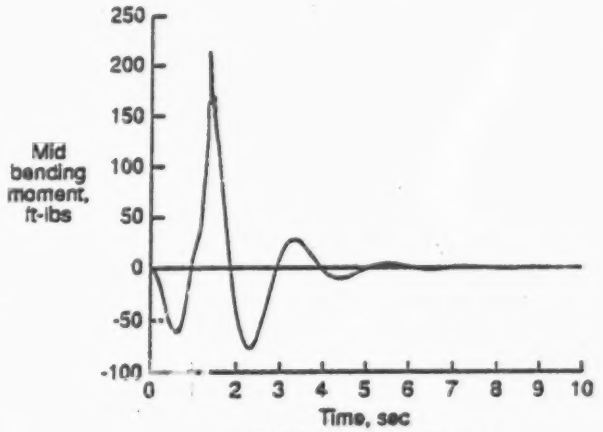

(b) Mid bending moment

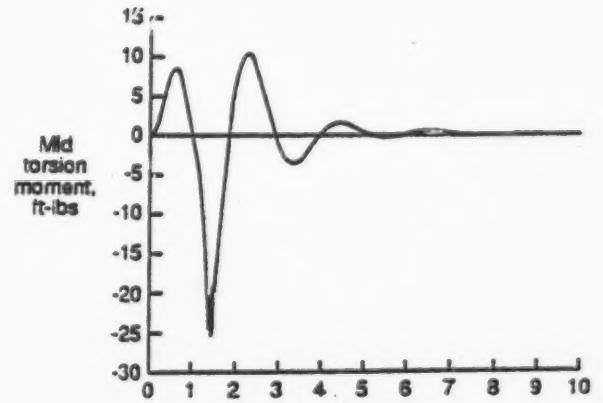

(c) Mid torsion moment

Figure 8. - Time-correlated gust loads from SDG Method 2.

NASA

Report Documentation Page

1. Report No.	2. Government Accession No.	3. Recipient's Catalog No.
NASA TM-101571		

4. Title and Subtitle

An Investigation of the "Overlap" Between the Statistical Discrete Gust and the Power Spectral Density Analysis Methods

5. Report Date

April 1989

6. Performing Organization Code

7. Author(s)

Boyd Perry III, Anthony S. Pototzky, Jessica A. Woods

8. Performing Organization Report No

10. Work Unit No.

505-63-21-04

9. Performing Organization Name and Address

NASA Langley Research Center
Hampton, VA 23665-5225

11. Contract or Grant No

13. Type of Report and Period Covered

Technical Memorandum

12. Sponsoring Agency Name and Address

National Aeronautics and Space Administration
Washington, DC 20546-0001

14. Sponsoring Agency Code

15. Supplementary Notes

Presented at the AIAA 30th Structures, Structural Dynamics and Materials Conference in Mobile, Alabama, April 3-5, 1989.

16. Abstract

This paper presents the results of a NASA investigation of a claimed "Overlap" between two gust response analysis methods: the Statistical Discrete Gust (SDG) and the Power Spectral Density (PSD) Method. The claim is that the ratio of an SDG response to the corresponding PSD response is 10.4. Analytical results presented in this paper for several different airplanes at several different flight conditions indicate that such an "Overlap" does appear to exist. However, the claim was not met precisely: a scatter of up to about 10% about the 10.4 factor can be expected.

17. Key Words (Suggested by Author(s))

Gust Loads Analysis Methods
Statistical Discrete Gust (SDG) Method
Power Spectral Density (PSD) Method
SDG-PSD Overlap

18. Distribution Statement

Unclassified - Unlimited

Subject Category - 05

19. Security Classif. (of this report)	20. Security Classif. (of this page)	21. No. of pages	22. Price
Unclassified	Unclassified	13	A03

NASA FORM 1626 OCT 86